Environment International 210 (2026) 110213

Contents lists available at ScienceDirect

Environment International

journal homepage: www.elsevier.com/locate/envint

Short communication

Mapping the impact of prolonged microplastics exposure on enteric viral infections using human intestinal organoids

Jiangrong Zhou [a], Yilan Zhao [a], Xincheng Li [a,b], Guige Xu [c], Marcel J.C. Bijvelds [a], Luc J.W. van der Laan [b], Annemarie C. de Vries [a], Qiuwei Pan [a], Pengfei Li [a,*]

[a] Department of Gastroenterology and Hepatology, Erasmus MC, University Medical Center, Rotterdam, the Netherlands
[b] Department of Surgery, Erasmus MC Transplant Institute, Erasmus MC, University Medical Center, Rotterdam, the Netherlands
[c] Department of Preventive Veterinary Medicine, College of Veterinary Medicine, Shandong Agricultural University, Taian, Shandong, China

ARTICLE INFO

Keywords:
Microplastics
Nanoplastics
Intestinal organoids
Exposome
Enteric viral infection
Antiviral treatment

ABSTRACT

Micro- and nanoplastic particles (MNPs) are pervasive environmental pollutants increasingly detected in the human body, yet the health consequences of chronic exposure remain poorly defined. Human intestinal organoids (HIO) have emerged as superior platforms for modelling intestinal diseases including enteric viral infections. In this study, we established a chronic MNPs exposure model using HIO. Long-term MNPs exposure elicited transcriptomic signatures of mitochondrial stress and broad metabolic disruption without inducing overt epithelial cell death. Using this system, we modeled enteric viral infection with echovirus and rotavirus, and demonstrated that prolonged MNPs exposure reprogrammed epithelial antiviral responses, altered viral infection capability, and diminished the efficacy of antiviral treatment. Together, these findings suggest that chronic microplastic exposure can reshape mucosal physiology, modulate virus-host interactions, and impair therapeutic responsiveness, highlighting an under recognized dimension of MNPs impact on infectious disease outcomes.

1. Introduction

Plastic products have become indispensable in modern society, yet their persistent waste has been posing substantial environmental challenges to the globe. Micro- and nanoplastic particles (MNPs), defined as small plastic fragments less than 5 mm in size, arise from the degradation of larger plastic products or from direct industrial production (Thompson et al., 2024). Their minute size, chemical stability, and resistance to biodegradation enable prolonged environmental persistence and progressive accumulation. Consequently, MNPs are now detected across nearly all ecological compartments, including marine and water systems, soil, air, and even in the human food chain (Kosuth et al., 2018; O'Brien et al., 2023; Sajjad et al., 2022; Zhang et al., 2016). This ubiquitous presence leads to inevitable and lifelong human exposure, with recent evidence demonstrating MNPs bioaccumulation across multiple organ systems in humans (Ali et al., 2024; Nihart et al., 2025).

Ingestion constitutes a major route of human exposure to MNPs (Lamoree et al., 2025; van der Laan et al., 2023). Once entering the gastrointestinal tract through contaminated food or water, these small particles directly interact with the intestinal epithelium, where they can accumulate and induce sustained oxidative stress, barrier disfunction and potential inflammation (Dutta et al., 2025; Hirt and Body-Malapel, 2020). Emerging clinical observations have further linked MNPs with increased inflammatory bowel disease activity, suggesting that chronic exposure may exacerbate underlying intestinal pathology (Yan et al., 2022). Meanwhile, over the past decade, growing attention has focused on the interactions between MNPs and environmental pathogens including bacteria and viruses. Experimental studies have demonstrated that MNPs can act as vectors for viruses, prolong viral stability (Lu et al., 2022), and under certain conditions, enhance viral infectivity (Wang et al., 2023; Zhang et al., 2022), thereby amplifying their public health relevance. The intestinal epithelium serves as a primary entry and replication site for numerous enteric viruses. Enteroviruses, for example, initiate infection in the gut before disseminating systemically, leading to illness ranging from mild febrile disease to severe neurological complications. Rotavirus (RV), another major enteric pathogen, account for

Abbreviations: CTR-M, mock-infected controls; CTR-E1, control organoids infected with EV1; CTR-E1-P, EV1-infected control organoids treated with pleconaril; MNPs-M, mock-infected organoids exposed to MNPs; MNPs-E1, MNPs-exposed organoids infected with EV1; MNPs-E1-P, EV1-infected, MNPs-exposed organoids treated with pleconaril.

* Corresponding author.
E-mail address: p.li@erasmusmc.nl (P. Li).

https://doi.org/10.1016/j.envint.2026.110213
Received 18 January 2026; Received in revised form 1 March 2026; Accepted 22 March 2026
Available online 23 March 2026

more than 250 million infections annually in children and remain one of the leading causes of diarrhea-related mortality worldwide (Troeger et al., 2018; Xu et al., 2025). In this context, ingested MNPs may act as vectors for enteric viral transmission and facilitate their entry into human and animal intestines. However, whether ingested MNPs that accumulate within human body, particularly within the intestinal epithelium, would modulate virus infection remains largely unknown.

The advent of organoid technology has provided advanced platforms for investigating communicable and non-communicable diseases. Primary organoids are self-organized three-dimensional cultures that are derived from tissue-resident stem cells. They encompass key aspects of native tissue architecture, cellular diversity, and physiological function in comparison with traditional two-dimensional cell lines (Sato et al., 2009). Since the COVID-19 pandemic, organoid systems have been increasingly adopted to model emerging and re-emerging viral diseases, for example recapitulating echovirus (EV) and RV infections in intestinal organoids (Xu, et al., 2025; Yin et al., 2015). More recently, organoid-based models have also been applied to MNPs research, in particular for evaluating tissue-specific toxicity across different organ systems (Cong et al., 2024). Given the unique advantages of organoids in modeling viral infection and environmental toxicants, we reasoned that they provide an ideal platform for probing whether chronic exposure to MNPs alters host susceptibility to viral infection.

In this study, we established a chronic MNPs exposure model using human intestinal organoids (HIOs), followed by infection with representative enteric viruses, including enteroviruses and rotavirus. Using this platform, we delineated how sustained MNPs exposure reshapes virus–host interactions within the intestinal epithelium. Furthermore, we evaluated whether chronic exposure to MNPs alters the efficacy of antiviral therapies against enteric viral infection.

2. Materials and methods

2.1. Intestinal organoids culture

Intestinal organoids were established as described previously (Bijvelds et al., 2022), and were maintained in expansion medium consisting of Advanced DMEM/F12 (Invitrogen) supplemented with penicillin–streptomycin (1%; Life Technologies), HEPES (10 mM), GlutaMAX (1×), N2 (1×), B27 (1×) (all Invitrogen), and N-acetylcysteine (1 μM; Sigma). The medium additionally contained the following growth factors and small molecules: mouse EGF (50 ng/mL), Wnt3a conditioned medium (50%), noggin conditioned medium (10%), Rspondin-1 conditioned medium (20%), nicotinamide (10 μM; Sigma), gastrin (10 nM; Sigma), A83-01 (500 nM; Tocris), and SB202190 (10 μM; Sigma). Medium was refreshed every 2–3 days, and cultures were passaged at a 1:4 ratio every 6–7 days. Use of human intestinal tissue was approved by the Medical Ethical Council with informed consent (MEC-2021-0432; MEC-2023-0629).

2.2. Exposure of intestinal organoids to MNPs

Fluorescent and nonfluorescent MNPs of different sizes were used in this study. Fluoresbrite YG 100-nm polystyrene nanoparticles (Cat. No. 16662-10; Polysciences) were supplied as a 2.5% aqueous suspension. Nonfluorescent 5-μm polystyrene microparticles (Cat. No. 79633-10ML-F; Merck Life Science) were supplied as a 10% aqueous suspension, whereas fluorescent 5-μm polystyrene microparticles (Cat. No. DCFG-L011; CD Bioparticles) were provided as a 1% aqueous suspension. All stock solutions were diluted in organoid expansion medium and vortexed immediately before use.

HIO were cultured in Matrigel until > 75% confluence. Matrigel-grown organoids exhibit inverted epithelial polarity, limiting MNPs access to the apical surface (Lee et al., 2024). Existing alternatives, such as monolayers or apical-out organoids, permit apical exposure but are suboptimal for long-term modeling or require specialized equipment (Cheng et al., 2022; Co et al., 2021). To overcome these limitations, organoids were collected, mechanically fragmented, and resuspended in expansion medium containing MNPs or in MNPs-free medium (control). Suspensions were mixed with Matrigel (2:8, v/v) and seeded. After polymerization, cultures were maintained in expansion medium replaced every 2 days, with MNPs exposure reapplied at each passage (every 6–7 days). A concentration of 300 μg/mL was selected based on prior studies showing efficient microplastic uptake with minimal cytotoxicity (Koner et al., 2025). After exposure, the organoids are collected for following experiments, as described below.

2.3. Cell lines and viruses

A549 human alveolar epithelial cells and MA-104 African green monkey kidney cells were maintained in DMEM (Lonza) supplemented with heat-inactivated fetal calf serum (10%; Sigma), penicillin (100 IU/mL), and streptomycin (100 μg/mL; Gibco). Echovirus 1 (EV1; GenBank AF029859) and echovirus 6 (EV6; JQ929657) were propagated in A549 cells, and RV strain SA11 (X16830) in MA-104 cells. Viral supernatants were harvested upon cytopathic effect, clarified, aliquoted, and stored at −80 °C. All cell lines were genotyped and confirmed mycoplasma-free.

2.4. Virus inoculation

Organoids, with or without prior chronic MNPs exposure, were mechanically fragmented and inoculated with RV, EV1, or EV6 for 2 h at 37 °C. To establish the acute exposure condition, viruses and MNPs (300 μg/mL) were added concurrently to the organoids and incubated for 2 h. Infections were carried out using approximately 4×10^4 PFU of RV or 2×10^4 PFU of EV. RV stocks were pre-activated with 0.05% trypsin for 10 min at 37 °C prior to inoculation. To enhance infection efficiency, the organoid-virus suspensions were gently resuspended every 30 min during the incubation period. After inoculation, samples were centrifuged at 800 rpm for 5 min at 4 °C, the supernatant was removed, and pellets were washed three times with Advanced DMEM/F12 to eliminate residual viral particles. Infected organoids were then seeded into wells and cultured for 48 h before downstream analyses.

2.5. Immunofluorescence staining and confocal imaging

Organoids were fixed in 4% PFA for 15 min, permeabilized with 0.2% Triton X-100 for 10 min, and washed with PBS. Samples were blocked (5% donkey serum, 1% BSA, 0.2% Triton X-100) for 1 h and incubated overnight at 4 °C with anti-EpCAM (1:500, rabbit) and double-stranded RNA (dsRNA; 1:500, mouse). After PBS washes, organoids were incubated for 1 h at room temperature with secondary antibodies (1:1000), including Alexa Fluor® 594-conjugated anti-mouse IgG (H + L) and Alexa Fluor® 647-conjugated anti-rabbit IgG (H + L). Nuclei were stained with DAPI, and images were acquired using a Leica SP8 confocal microscope.

2.6. RNA extraction and qRT-PCR

Total RNA was extracted using the NucleoSpin RNA II Kit (Bioke, Netherlands) and quantified by NanoDrop ND-1000 spectrophotometer (Wilmington, USA). Gene expression was quantified by SYBR Green-based qRT-PCR using the Applied Biosystems SYBR Green PCR Master Mix (Thermo Fisher Scientific) on a StepOnePlus Real-Time PCR System (Thermo Fisher Scientific). Glyceraldehyde 3-phosphate dehydrogenase (GAPDH) served as the housekeeping gene for normalization. Relative expression levels were calculated using the 2ˆ−ΔΔCT method (ΔΔCT = ΔCT_sample − ΔCT_control).

2.7. Cytotoxicity measurement

Cell viability was assessed using AlamarBlue according to the

manufacturer's instructions. Virus-induced cytopathic effects were visualized by propidium iodide (PI) staining (Fisher Scientific) and quantified by lactate dehydrogenase (LDH) release using the CytoTox 96® Non-Radioactive Cytotoxicity Assay (Promega), following the manufacturer's protocol.

2.8. Genome-wide RNA sequencing and data analysis

Organoids with or without MNPs exposure were infected with EV1 as described above and harvested at 48 h post-infection. For antiviral treatment, infected organoids were exposed to 0.1 μM pleconaril starting 1 h post-infection and maintained until 48 h post-infection. In parallel, uninfected organoids were cultured under identical conditions as negative controls. Total RNA was extracted using the Macherey-Nagel NucleoSpin RNA II Kit (Bioke, Netherlands) and quantified by NanoDrop ND-1000 spectrophotometer (Wilmington, USA). RNA sequencing was performed by Novogene using a paired-end 150 bp (PE150) strategy.

2.9. Statistics

Statistical analyses were performed using GraphPad Prism 8 (GraphPad Software, San Diego, USA). Data are presented as the mean ± standard error of the mean (SEM). Two-group comparisons were assessed using a two-tailed Mann-Whitney test, and comparisons among three or more groups were performed using the Kruskal-Wallis test with Dunn's test. Asterisks indicate statistical significance relative to the control group (*$P < 0.05$; **$P < 0.01$; ***$P < 0.001$).

3. Results

3.1. Establishment and characterization of chronic MNPs exposure in HIO

Polystyrene (PS), extensively used in food packaging and disposable consumer products, is a dominant contributor to environmental plastic waste and a key source of human MNPs exposure (Cassidy and Elyashiv-Barad, 2007; Wang et al., 2023). To model long-term MNPs exposure, we continuously treated HIO with PS-MNPs of either 100 nm or 5 μm size (Fig. 1A). During the exposure process, we observed that MNPs with 100 nm size exhibited pronounced *peri*-organoid clustering, whereas 5 μm MNPs showed a more diffuse distribution (Fig. 1B). Confocal microscopy revealed internalization of 100 nm MNPs within organoid cells (Fig. 1C), but 5 μm MNPs remained extracellular (Supplementary Fig. 1A). Morphologically, intestinal organoids preserved intact and normal appearance, with cell viability not influenced after four weeks of MNPs exposure (Fig. 1D; Supplementary Fig. 1B). Nevertheless, transmission electron microscopy (TEM) revealed ultrastructural alterations in MNPs-exposed organoids compared to non-exposed organoids (Fig. 1E; Supplementary Fig. 1C). For example, 100 nm MNPs-exposed organoids exhibited reduced cytoplasmic electron density, pronounced mitochondrial cristae dilation with small vacuoles (red arrowheads), and mild rough endoplasmic reticulum (RER) cisternal widening accompanied by partial ribosome loss (white arrowheads). In contrast, these alterations were minimal or absent in organoid treated with 5 μm MNPs. Based on these observations, 100 nm MNPs were selected for subsequent analyses.

To further characterize host responses to MNPs exposure, genome-wide transcriptomic profiling was performed. Principal component analysis (PCA) clearly separated MNPs-exposed from non-exposed intestinal organoids (Supplementary Fig. 1D). Differential expression genes (DEGs) analysis identified 177 genes uniquely expressed genes in MNPs-exposed organoids, whereas over 11,000 genes were shared between both groups (Fig. 1F). Volcano plot analysis revealed 1,330 upregulated and 1,358 downregulated genes ($p < 0.05$) upon chronic exposure to MNPs (Supplementary Fig. 1E). Intriguingly, a cascade of upregulated genes such as DHRS9, REG4, DUOXA2, MMP1, and SLC2A3 are associated with epithelial barrier integrity, oxidative stress responses, and metabolic regulation. Gene set enrichment analysis (GSEA) further revealed significant enrichment of fat digestion and absorption, and peroxisome (Fig. 1G-H). Likewise, sankey diagram visualized the most significantly regulated genes within enriched gene ontology (GO) biological processes, including organic hydroxy compound metabolic process, lipid transport, lipid localization, alcohol metabolic process, and organic anion transport (Fig. 1I). Collectively, these findings demonstrate that chronic exposure to MNPs elicits physiological and transcriptional alterations in HIO.

3.2. Chronic MNPs exposure affects enteric virus infection and disturbs the host-virus transcriptional response

To map the role of MNPs during viral infection process, we co-inoculated the virus and MNPs with intestinal organoids. Three enteric viruses, EV1, EV6, and RV, were respectively tested. Interestingly, co-inoculation of MNPs with EV1 or EV6 in intestinal organoids resulted in enhanced viral infectivity compared with organoids inoculated with EV1 or EV6 alone (Supplementary Fig. 2A-B). Differently, co-inoculating RV and MNPs in organoids reduced the infection efficacy compared to inoculating RV alone (Supplementary Fig. 2C). However, human intestinal epithelium is constantly exposed to MNPs, whereas viral infection generally occurs independently without simultaneous MNPs involvement, making it essential to determine how post chronic MNPs exposure alters viral infection dynamics. To model this scenario, intestinal organoids were firstly exposed to MNPs for four-weeks, then EV1 and RV were used to inoculate the organoids (Fig. 2A). Unexpectedly, prior chronic exposure to MNPs significantly attenuated EV1 infection, as demonstrated by reduced viral RNA levels quantified by qRT-PCR (Fig. 2B). $TCID_{50}$ assay showed lower infectious titers in MNPs treated organoids (Fig. 2C). Similar to EV1, the infection efficacy of RV dramatically decreased in MNPs-treated organoids (Fig. 2D-E). Consistently, MNPs exposure also mitigated virus-induced cytopathic effects in organoids (Fig. F-G, Supplementary Fig. 3A). Immunofluorescence staining of viral dsRNA demonstrated abundant virus replicating signal in non-exposed organoids, whereas MNPs-exposed organoids showed substantially diminished dsRNA signal (Fig. 2H; Supplementary Fig. 3B). Moreover, the virus signal was identified to colocalize with MNPs in organoid cells (Fig. 2H, orange arrowheads). Collectively, acute co-exposure of MNPs induces different effects on the infection efficacy of EV1 and RV, whereas chronic pre-exposure of MNPs suppresses the infection by both viruses, underscoring that MNPs–virus interactions are shaped by both exposure condition and virus species.

To assess how chronic MNPs exposure reshapes virus-host interactions, we performed transcriptomic profiling of EV1-infected and uninfected intestinal organoids with or without exposure to MNPs. Venn diagram analysis showed a substantially reprogramed host response to EV1 infection following chronic MNPs exposure, with 1,530 DEGs uniquely detected in MNPs-exposed organoids and 3,070 DEGs unique to non-exposed controls (Fig. 3A). In control organoids, volcano plot analysis indicated a robust antiviral response to EV1 infection, characterized by marked induction of interferon-stimulated genes (e.g., OASL, IFIT2, ISG15), while metabolism and cell survival related genes were downregulated (Fig. 3B). In contrast, EV1 infection in MNPs-exposed organoids also triggered antiviral responses, albeit with reduced magnitude. Notably, genes involved in key metabolism processes (PSAT1, SLC2A3, SLC7A5), antioxidant defense (PRDX3, UCP2), and stem cell maintenance (LRIG1, CDCA7) were dramatically downregulated, suggesting exacerbated metabolic suppression and impaired regenerative capacity (Fig. 3C). Consistent with these findings, GO enrichment analysis showed activation of antiviral and inflammatory pathways following EV1 infection in both conditions, while chronic MNPs exposure was additionally associated with enrichment of apoptosis and cell-death associated pathways (Fig. 3D). Moreover,

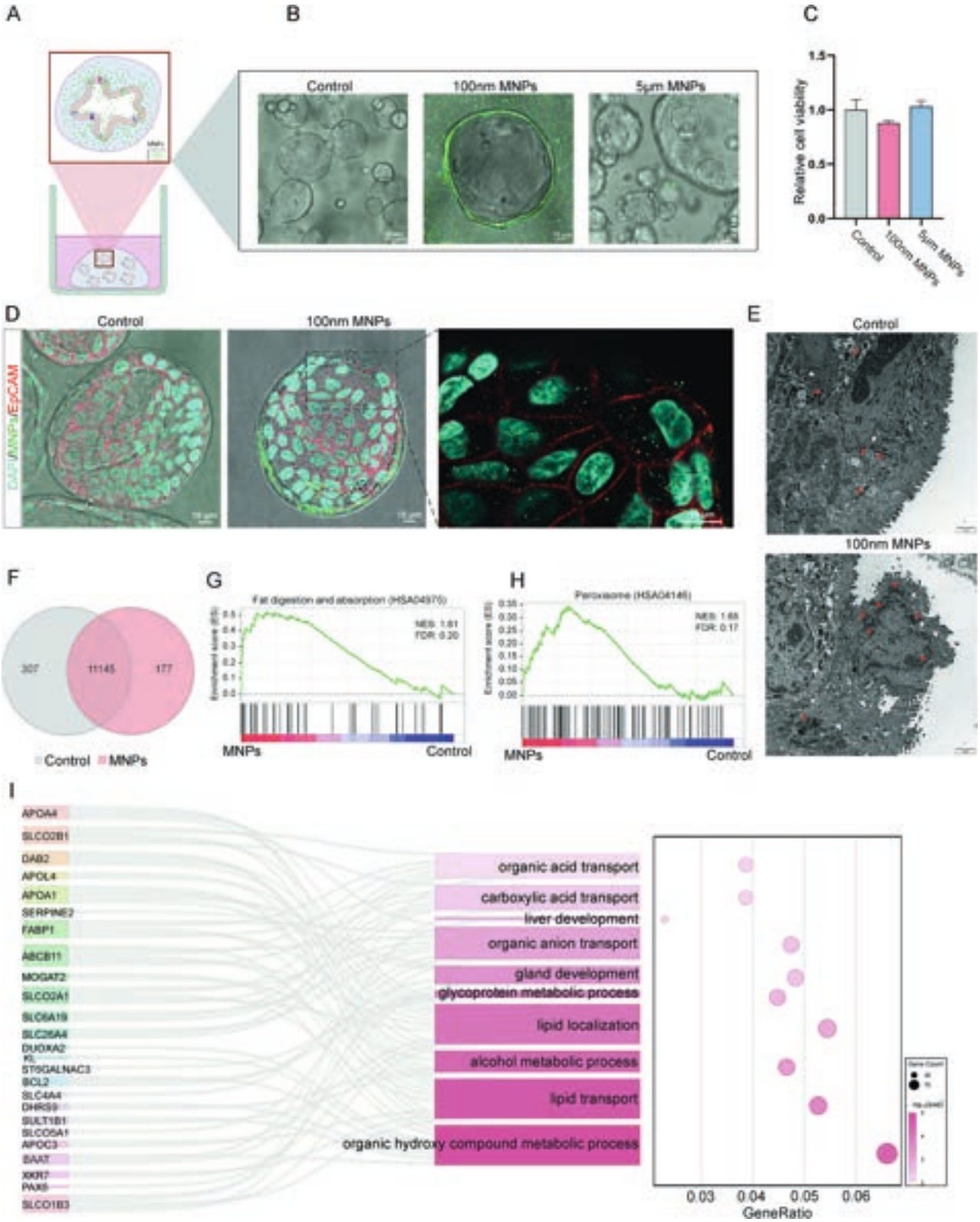

Fig. 1. Morphological and transcriptomic effects of chronic MNPs exposure in HIO. (A) Schematic of chronic PS-MNPs exposure; (B) confocal images of organoids co-cultured with 100 nm MNPs (scale bar = 10 μm) or 5 μm MNPs (green; scale bar = 50 μm); (C) representative confocal images showing internalization of 100 nm fluorescently labeled MNPs (scale bar = 10 μm); (D) relative viability after 4 weeks of MNPs exposure, with fluorescence intensity measured at λ_Exc 530 nm / λ_Em 590 nm; (E) representative TEM images showing that control organoids exhibit intact epithelial ultrastructure with normal mitochondria (red arrowheads) and rough endoplasmic reticulum (RER; white arrowheads), whereas 100 nm MNPs-exposed organoids display reduced cytoplasmic density and abnormal mitochondria and RER; (F) Venn diagram showing 177 DEGs unique to 100 nm MNPs-exposed organoids and 307 unique to controls; (G-H) GSEA showing regulation of the fat digestion and absorption (G) and peroxisome (H) in MNPs-exposed organoids compared to control organoids: (I) Sankey diagram depicting the linkage between significantly altered genes (left) and the top 10 enriched GO terms (right) in 100 nm MNPs-exposed organoids versus controls. (For interpretation of the references to colour in this figure legend, the reader is referred to the web version of this article.)

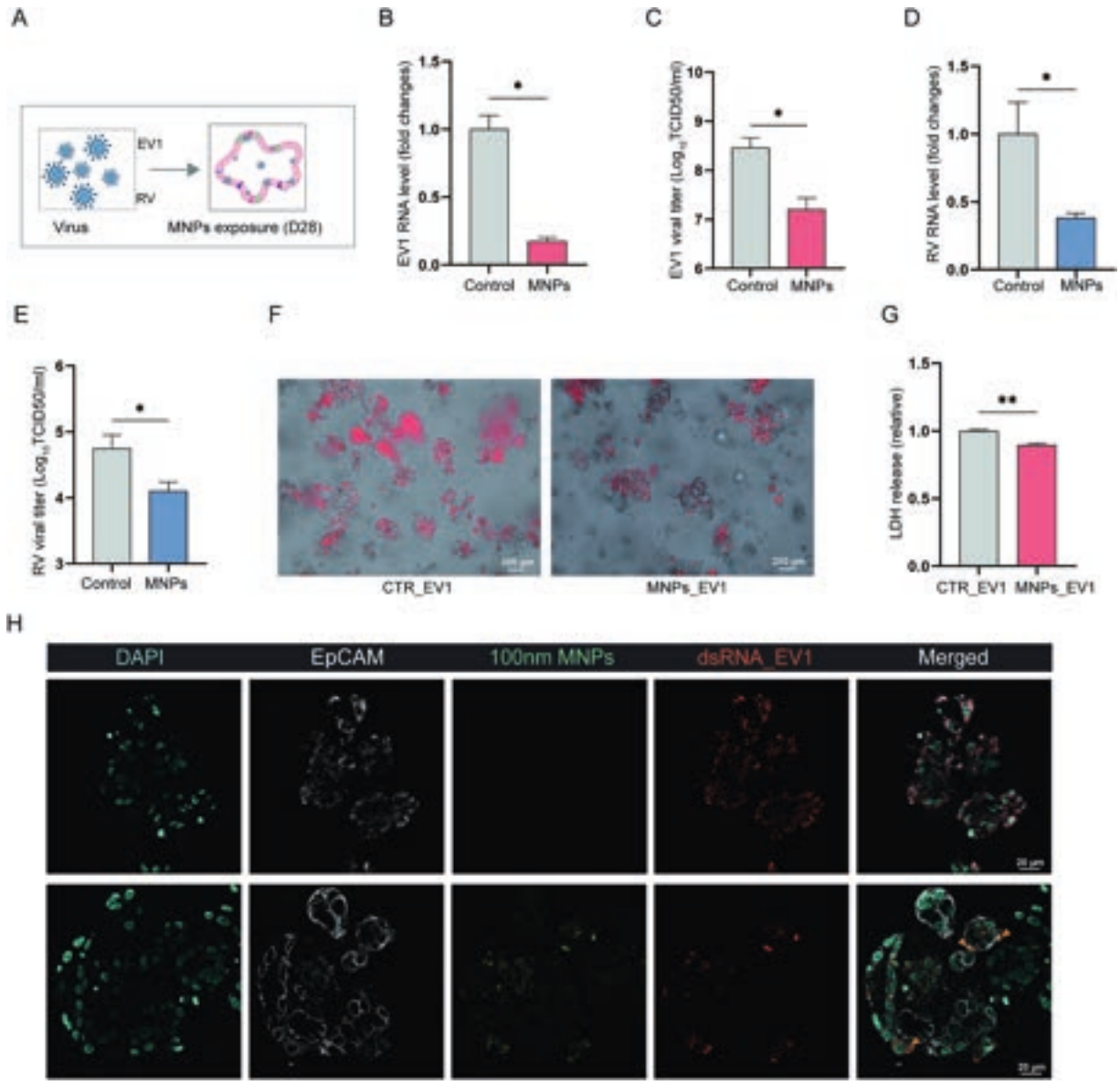

Fig. 2. Chronic MNPs exposure interferes with virus infection. (A) Schematic of chronic 100 nm MNPs exposure followed by viral infection; (B-C) qRT-PCR quantification of EV1 RNA levels (B) and infectious viral titers (C) (n = 4 biological replicates); (D-E) qRT-PCR quantification of RV RNA levels (D) and infectious viral titers (E) (n = 4 biological replicates); (F) PI staining showing EV1-induced cell death (scale bar = 200 μm); (G) quantification of LDH release (n = 4 biological replicates); (H) confocal images of viral dsRNA in EV1-infected organoids at 48 h post infection, with orange arrowheads indicating co-localization of EV1 dsRNA and 100 nm MNPs (scale bar = 20 μm). Data are presented as mean ± SEM. Statistical significance was assessed using a two-tailed Mann-Whitney *U* test (* $p < 0.05$, ** $P < 0.01$). (For interpretation of the references to colour in this figure legend, the reader is referred to the web version of this article.)

pathways involved in DNA double-strand break repair, energy metabolism, and precursor metabolite generation were selectively downregulated in MNPs-exposed organoids (Fig. 3D), highlighting profound disruption of cellular homeostasis and metabolic competence.

3.3. Chronic MNPs exposure attenuates antiviral treatment responsiveness

Since chronic exposure of MNPs in intestinal organoids reprogrammed host responses to virus infections, we next investigated whether MNPs exposure would influence the efficacy of antiviral treatment. Pleconaril, a clinically used drug for treating enterovirus infections, was tested in intestinal organoids. QRT-PCR quantification showed a dose-dependent inhibition to EV1 RNA level in both MNPs-exposed and non-exposed organoids (Supplementary Fig. 4A-B). Strikingly, pleconaril treatment inhibited approximately 70% viral RNA in MNPs-exposed organoids, whereas over 99% viral RNA was blocked in organoids without MNPs exposure (Fig. 4A).

RNA sequencing demonstrated a marked reduction in EV1 transcripts in pleconaril-treated compared to untreated organoids and likewise, more viral transcripts were mapped in MNPs-exposed organoids compared to non-exposed organoids (52% versus 38%) (Fig. 4B). In-depth analysis revealed abundantly expressed transcripts mapped to different regions of the EV1 reference genome, and importantly, chronic MNPs exposure was associated with less viral transcript reduction following pleconaril treatment (Fig. 4C). Consistently, heatmap analysis of DEGs showed that pleconaril treatment partially restored the EV1-induced transcriptional profile towards the uninfected state in both conditions, however, this restorative effect was attenuated in MNPs-exposed organoids (Supplementary Fig. 5; Supplementary Fig. 6). In parallel, gene set variation analysis (GSVA) revealed persistent perturbation of metabolic pathway activity in MNPs-exposed organoids

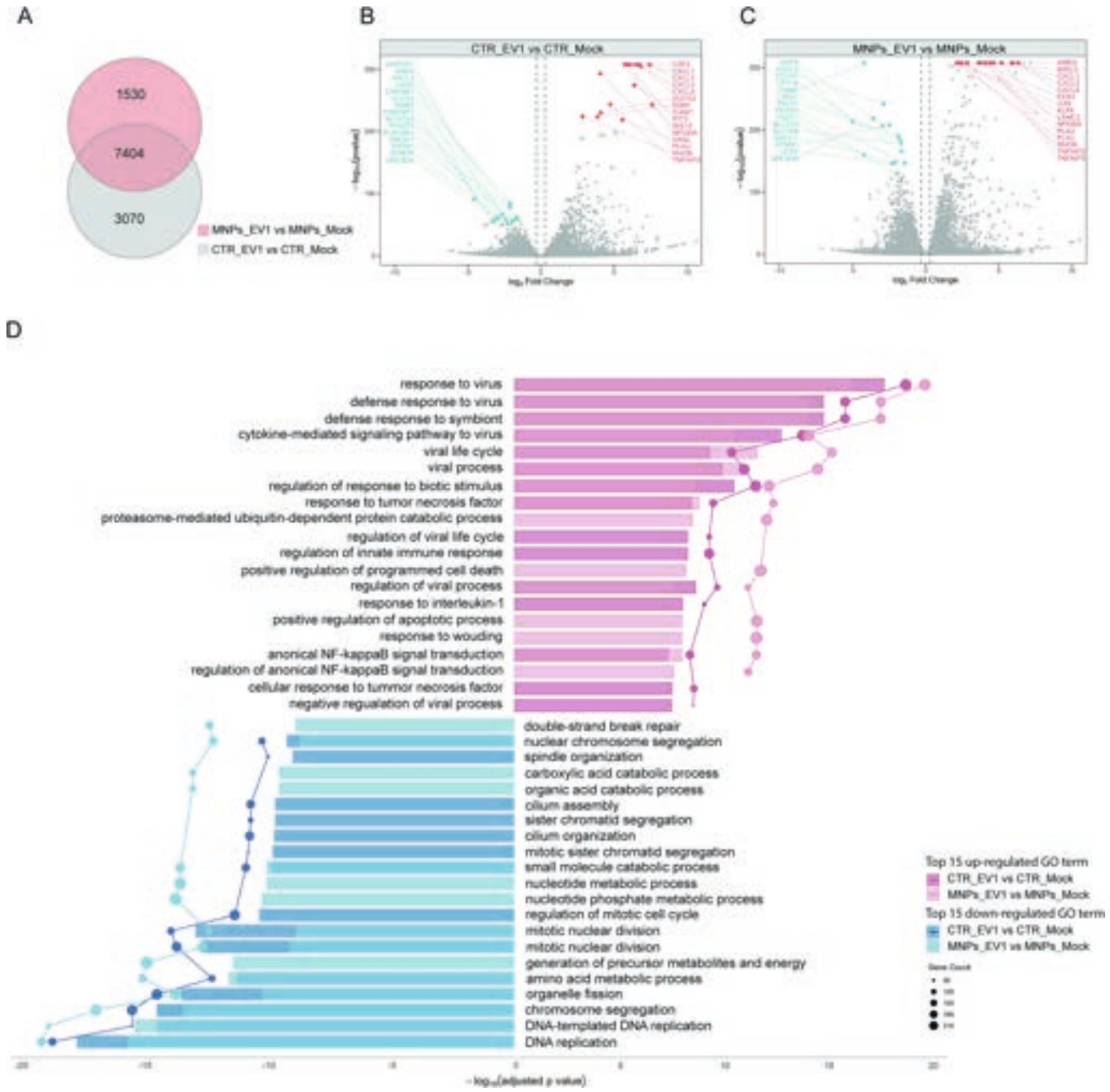

Fig. 3. Chronic MNPs exposure disrupts host–virus transcriptional responses. (A) Venn diagram of unique DEGs, (B-C) volcano plot of significantly upregulated and downregulated DEGs, and (D) top 15 significantly enriched GO terms in EV1-infected MNPs-exposed and control organoids relative to their corresponding uninfected organoids (n = 4 biological replicates).

despite antiviral treatment (Fig. 4D–E; Supplementary Fig. 7). Collectively, these findings suggest that chronic MNPs exposure compromises the efficacy of antiviral treatment against enteric viral infection.

4. Discussion

MNPs have rapidly emerged as global contaminants, yet their long-term physiological impact remains poorly defined. Currently, most understandings to MNPs are from acute or short-term MNPs exposure studies, which *de facto* not reflect the chronic, low-dose exposure experienced by humans. In this study, we exquisitely established prolonged MNPs exposure in HIO and further investigated enteric viral infections in this model. We extensively characterized the impact of chronic MNPs exposure to host physiology, virus-host interactions, and antiviral treatment.

Organoid systems have recently proven valuable for dissecting MNPs-induced toxicity, as they can better recapitulate the original characteristics of tissues and organs compared to conventional cell models (Cheng et al., 2024; Park et al., 2023). Consistent with prior work, we observed that nano-scale PS particles, but not larger microplastics, were internalized into organoid cells, highlighting particle size as a critical determinant of biological impact (Chen et al., 2020; Lu et al., 2022; Shen et al., 2022). Although we did not directly trace the subcellular localization of MNPs, ultrastructural observations revealed mitochondrial cristae dilation, vacuolization, and RER alterations, accompanied by transcriptional signatures of oxidative stress and

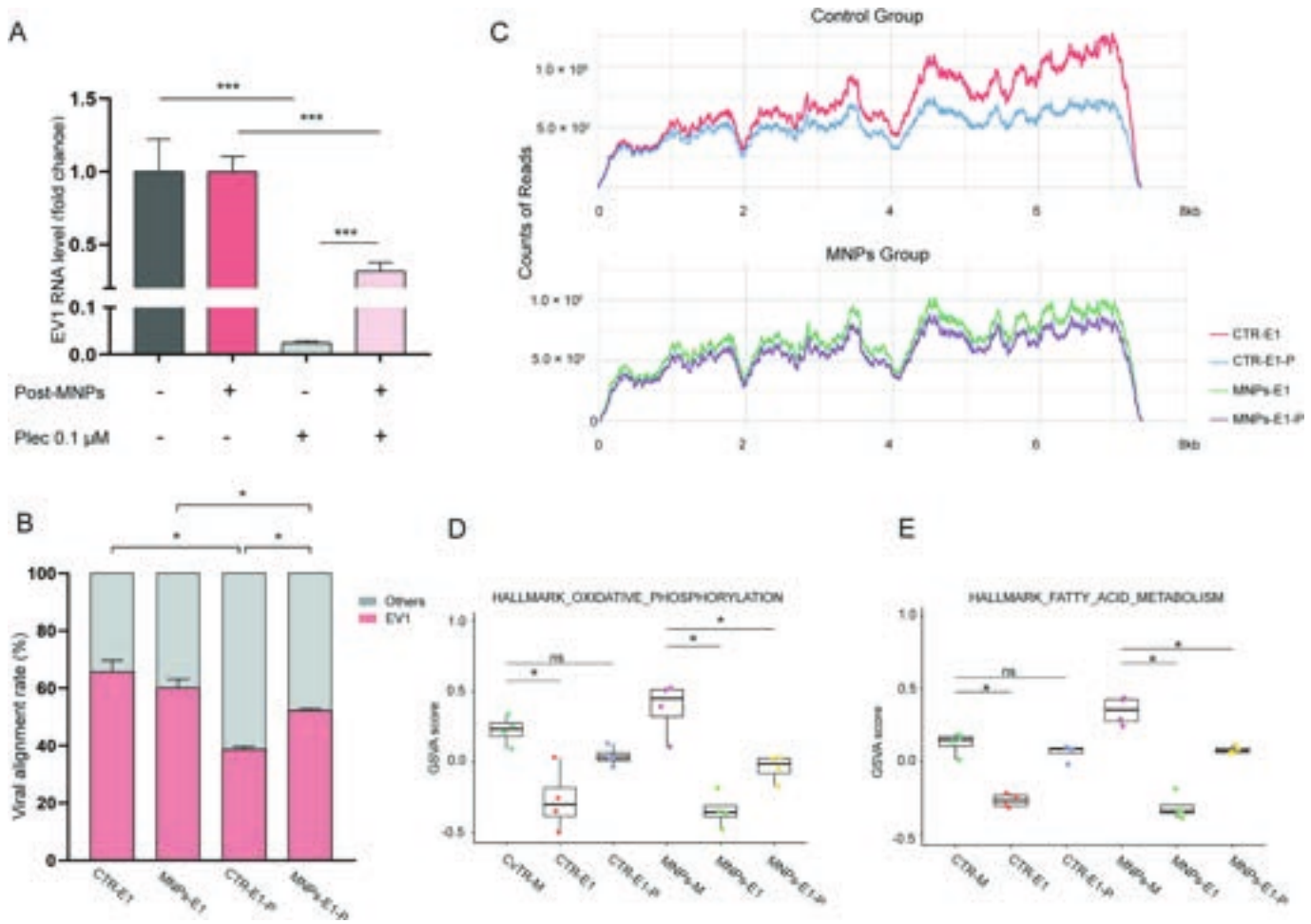

Fig. 4. Chronic MNPs exposure attenuates antiviral treatment responsiveness. (A) Quantification of viral RNA level in EV1-infected MNPs-exposed and control organoids with or without 0.1 μM pleconaril (plec) treatment for 48 h (n = 8 biological replicates); overall alignment rates of viral reads to the EV1 genome (B) and read depth across the EV1 genome (C) in infected MNPs-exposed and control organoids with or without plec treatment (n = 4 biological replicates). (D-E) box plots show GSVA enrichment scores for Hallmark oxidative phosphorylation (D), and fatty acid metabolism (E) across the indicated organoid groups. Each dot represents an individual sample. Data are presented as mean ± SEM. Statistical significance was assessed using a two-tailed Mann-Whitney *U* test (*p < 0.05, ***p < 0.001).

metabolic perturbation. In line with our findings, metabolic disruptions including ROS accumulation and loss of mitochondrial potential, have been also observed in mouse intestinal organoids exposed to MNPs (Xuan et al., 2024). Moreover, multiple studies have suggested mitochondrial vulnerability to MNPs exposure in different species (Jeong et al., 2016; Qin et al., 2022). Collectively, MNPs are capable to disrupt core metabolic and homeostatic processes essential for epithelial function.

Intestinal epithelium serves as the frontline barrier against enteric pathogens and the major site of MNPs accumulation. We postulate that MNPs exposure may modulate epithelial susceptibility to viral infection. Through modeling acute co-exposure conditions in intestinal organoids, we found that MNPs enhanced EV1 and EV6 infection efficacy, which is consistent with prior observations for other RNA viruses (Wang, et al., 2023; Zhang, et al., 2022). In contrast, co-exposure conditions suppressed RV infection, suggesting that the interaction between MNPs and viruses is not universally proviral. One potential explanation is that the two types viruses own distinct structure and size, which may confer disparate interaction affinities with microplastics thereby influencing viral infectivity (Zhang et al., 2022). We further investigated virus infections in organoids following chronic MNPs exposure, which is closer to the real-world scenario. Strikingly, the chronic exposure paradigm revealed an opposite phenomenon, with long-term MNPs exposure markedly attenuating the replication of both EV1 and RV. We next performed transcriptomic analysis to seek mechanistic clues for such distinct results. Although MNPs-exposed organoids mounted antiviral responses upon viral challenge, these responses were more dysregulated than those in control organoids. Importantly, this attenuated antiviral signaling was accompanied by decreased, rather than increased, viral replication. One possible explanation is that chronic MNPs exposure induces metabolic disturbance and oxidative stress, thereby constraining the capacity of host cells to support the bioenergetic and biosynthetic demands required for efficient viral replication (Khan et al., 2021; Kleinehr et al., 2025; Palmer, 2022). In addition, enrichment of cell death- and apoptosis-related pathways triggered by MNPs may further restrict viral propagation by promoting the elimination of infected cells.

On the other hand, our findings reveal that the consequences of chronic MNPs exposure extend beyond infection susceptibility to therapeutic responsiveness. Although pleconaril retained dose-dependent inhibitory activity against EV1 in both non-exposed and MNPs-exposed organoids, the later showed substantially diminished efficacy. Notably, transcriptomic analysis revealed no significant alterations in canonical xenobiotic metabolism or drug transport pathways (e.g., CYP/UGT enzymes or ABC/SLC drug transporters). Instead, GSVA indicated persistent perturbation of metabolic programs in MNP-exposed organoids, suggesting that the diminished pleconaril efficacy may arise indirectly from sustained host metabolic reprogramming and an altered epithelial physiological state. These observations raise important

concerns that environmental MNPs could compromise antiviral treatment outcomes, particularly for populations with continuous high-level exposure.

This study has several limitations. First, primary intestinal organoids lack immune and microbial components, all of which shape mucosal responses to pollutants and pathogens. Second, we focused on a single polystyrene particle type, while real-world exposures encompass heterogeneous shapes and chemistries that may exert distinct effects. Third, the use of Matrigel during organoids culture may partially limit direct contact between organoid cells and MNPs, which potentially results in a lower effective MNPs exposure than the normal culture condition without Matrigel. Finally, although our ultrastructural and transcriptomic findings implicate disruptions in metabolic and antiviral pathways by MNPs involvement, mechanistic validation will be essential to delineate the underlying processes.

In summary, we established chronic MNPs exposure in HIO for investigating the MNPs-host-virus interactions. Our findings demonstrate that chronic exposure of MNPs could alter intestinal epithelial function, influencing susceptibility to enteric viral infection while simultaneously diminishing antiviral drug efficacy.

CRediT authorship contribution statement

Jiangrong Zhou: Writing – original draft, Methodology, Investigation, Formal analysis, Data curation. **Yilan Zhao:** Writing – review & editing, Validation, Software, Investigation. **Xincheng Li:** Writing – review & editing, Visualization, Software. **Guige Xu:** Writing – review & editing, Methodology. **Marcel J.C. Bijvelds:** Writing – review & editing, Resources. **Luc J.W. van der Laan:** Writing – review & editing, Resources. **Annemarie C. de Vries:** Writing – review & editing, Resources. **Qiuwei Pan:** Writing – review & editing, Supervision, Methodology, Conceptualization. **Pengfei Li:** Writing – review & editing, Supervision, Methodology, Funding acquisition.

Declaration of competing interest

The authors declare that they have no known competing financial interests or personal relationships that could have appeared to influence the work reported in this paper.

Appendix A. Supplementary data

Supplementary data to this article can be found online at https://doi.org/10.1016/j.envint.2026.110213.

Data availability

Data will be made available on request.

References

Ali, N., Katsouli, J., Marczylo, E.L., Gant, T.W., Wright, S., Bernardino de la Serna, J., 2024. The potential impacts of micro-and-nano plastics on various organ systems in humans. Biomedicine 99, 104901. https://doi.org/10.1016/j.ebiom.2023.104901.

Bijvelds, M.J.C., Roos, F.J.M., Meijsen, K.F., et al., 2022. Rescue of chloride and bicarbonate transport by elexacaftor-ivacaftor-tezacaftor in organoid-derived CF intestinal and cholangiocyte monolayers. J. Cyst. Fibros. 21 (3), 537–543. https://doi.org/10.1016/j.jcf.2021.12.006.

Cassidy, K., Elyashiv-Barad, S., 2007. US FDA's revised consumption factor for polystyrene used in food-contact applications. Food Addit. Contam. 24 (9), 1026–1031. https://doi.org/10.1080/02652030701313797.

Chen, Y., Ling, Y., Li, X., Hu, J., Cao, C., He, D., 2020. Size-dependent cellular internalization and effects of polystyrene microplastics in microalgae P. helgolandica var. tsingtaoensis and S. quadricauda. J. Hazard. Mater. 399, 123092. https://doi.org/10.1016/j.jhazmat.2020.123092.

Cheng, W., Li, X., Zhou, Y., et al., 2022. Polystyrene microplastics induce hepatotoxicity and disrupt lipid metabolism in the liver organoids. Sci. Total Environ. 806, 150328. https://doi.org/10.1016/j.scitotenv.2021.150328.

Cheng, W., Chen, H., Zhou, Y., et al., 2024. Aged fragmented-polypropylene microplastics induced ageing statues-dependent bioenergetic imbalance and reductive stress: in vivo and liver organoids-based in vitro study. Environ. Int. 191, 108949. https://doi.org/10.1016/j.envint.2024.108949.

Co, J.Y., Margalef-Català, M., Monack, D.M., Amieva, M.R., 2021. Controlling the polarity of human gastrointestinal organoids to investigate epithelial biology and infectious diseases. Nat. Protoc. 16 (11), 5171–5192. https://doi.org/10.1038/s41596-021-00607-0.

Cong, J., Wu, J., Fang, Y., et al., 2024. Application of organoid technology in the human health risk assessment of microplastics: a review of progresses and challenges. Environ. Int. 188, 108744. https://doi.org/10.1016/j.envint.2024.108744.

Dutta, P., Rabeeah, S., Vargas, A., Oldfield ECt, Johnson, D.A., 2025. A comprehensive narrative review of potential gastrointestinal adverse effects from micro(nano) plastic exposure. Clin. Gastroenterol. Hepatol. https://doi.org/10.1016/j.cgh.2025.11.002.

Hirt, N., Body-Malapel, M., 2020. Immunotoxicity and intestinal effects of nano- and microplastics: a review of the literature. Part. Fibre Toxicol. 17 (1), 57. https://doi.org/10.1186/s12989-020-00387-7.

Jeong, C.B., Won, E.J., Kang, H.M., et al., 2016. Microplastic size-dependent toxicity, oxidative stress induction, and p-JNK and p-p38 activation in the monogonont rotifer (Brachionus koreanus). Environ. Sci. Technol. 50 (16), 8849–8857. https://doi.org/10.1021/acs.est.6b01441.

Khan, N.A., Kar, M., Panwar, A., et al., 2021. Oxidative stress specifically inhibits replication of dengue virus. J. Gen. Virol. 102 (4). https://doi.org/10.1099/jgv.0.001596.

Kleinehr, J., Bojarzyn, C.R., Schöfbänker, M., Daniel, K., Ludwig, S., Hrincius, E.R., 2025. Metabolic interference impairs influenza a virus replication by dampening vRNA synthesis. Npj Viruses. 3 (1), 22. https://doi.org/10.1038/s44298-025-00090-4.

Koner, S., Ramasubbu, S., Chandrasekaran, N., 2025. Toxicological profiling of polystyrene microplastics in raw 264.7 macrophages: linking microplastic exposure to immune cell impairment. Toxicology 517, 154239. https://doi.org/10.1016/j.tox.2025.154239.

Kosuth, M., Mason, S.A., Wattenberg, E.V., 2018. Anthropogenic contamination of tap water, beer, and sea salt. PLoS One 13 (4), e0194970. https://doi.org/10.1371/journal.pone.0194970.

Lamoree, M.H., van Boxel, J., Nardella, F., et al., 2025. Health impacts of microplastic and nanoplastic exposure. Nat. Med. 31 (9), 2873–2887. https://doi.org/10.1038/s41591-025-03902-5.

Lee, M.G., Lee, B.R., Lee, P., et al., 2024. Apical-out intestinal organoids as an alternative model for evaluating deoxynivalenol toxicity and Lactobacillus detoxification in bovine. Sci. Rep. 14 (1), 31373. https://doi.org/10.1038/s41598-024-82928-0.

Lu, Y.Y., Li, H., Ren, H., et al., 2022. Size-dependent effects of polystyrene nanoplastics on autophagy response in human umbilical vein endothelial cells. J. Hazard. Mater. 421, 126770. https://doi.org/10.1016/j.jhazmat.2021.126770.

Lu, J., Yu, Z., Ngiam, L., Guo, J., 2022. Microplastics as potential carriers of viruses could prolong virus survival and infectivity. Water Res. 225, 119115. https://doi.org/10.1016/j.watres.2022.119115.

Nihart, A.J., Garcia, M.A., El Hayek, E., et al., 2025. Bioaccumulation of microplastics in decedent human brains. Nat. Med. 31 (4), 1114–1119. https://doi.org/10.1038/s41591-024-03453-1.

O'Brien, S., Rauert, C., Ribeiro, F., et al., 2023. There's something in the air: a review of sources, prevalence and behaviour of microplastics in the atmosphere. Sci. Total Environ. 874, 162193. https://doi.org/10.1016/j.scitotenv.2023.162193.

Palmer, C.S., 2022. Innate metabolic responses against viral infections. Nat. Metab. 4 (10), 1245–1259. https://doi.org/10.1038/s42255-022-00652-3.

Park, S.B., Jung, W.H., Choi, K.J., Koh, B., Kim, K.Y., 2023. A comparative systematic analysis of the influence of microplastics on colon cells, mouse and colon organoids. Tissue Eng. Regen. Med. 20 (1), 49–58. https://doi.org/10.1007/s13770-022-00496-8.

Qin, J., Xia, P.F., Yuan, X.Z., Wang, S.G., 2022. Chlorine disinfection elevates the toxicity of polystyrene microplastics to human cells by inducing mitochondria-dependent apoptosis. J. Hazard. Mater. 425, 127842. https://doi.org/10.1016/j.jhazmat.2021.127842.

Sajjad, M., Huang, Q., Khan, S., et al., 2022. Microplastics in the soil environment: a critical review. Environ. Technol. Innov. 27, 102408. https://doi.org/10.1016/j.eti.2022.102408.

Sato, T., Vries, R.G., Snippert, H.J., et al., 2009. Single Lgr5 stem cells build crypt-villus structures in vitro without a mesenchymal niche. Nature 459 (7244), 262–265. https://doi.org/10.1038/nature07935.

Shen, R., Yang, K., Cheng, X., et al., 2022. Accumulation of polystyrene microplastics induces liver fibrosis by activating cGAS/STING pathway. Environ. Pollut. 300, 118986. https://doi.org/10.1016/j.envpol.2022.118986.

Thompson, R.C., Courtene-Jones, W., Boucher, J., Pahl, S., Raubenheimer, K., Koelmans, A.A., 2024. Twenty years of microplastic pollution research-what have we learned? Science 386 (6720). https://doi.org/10.1126/science.adl2746.

Troeger, C., Khalil, I.A., Rao, P.C., et al., 2018. Rotavirus vaccination and the global burden of rotavirus diarrhea among children younger than 5 years. JAMA Pediatr. 172 (10), 958–965. https://doi.org/10.1001/jamapediatrics.2018.1960.

van der Laan, L.J.W., Bosker, T., Peijnenburg, W., 2023. Deciphering potential implications of dietary microplastics for human health. Nat. Rev. Gastroenterol. Hepatol. 20 (6), 340–341. https://doi.org/10.1038/s41575-022-00734-3.

Wang, J., Lee, J., Kwon, E.E., Jeong, S., 2023. Quantitative analysis of polystyrene microplastic and styrene monomer released from plastic food containers. Heliyon 9 (5), e15787. https://doi.org/10.1016/j.heliyon.2023.e15787.

Wang, C., Wu, W., Pang, Z., et al., 2023. Polystyrene microplastics significantly facilitate influenza a virus infection of host cells. J. Hazard. Mater. 446, 130617. https://doi.org/10.1016/j.jhazmat.2022.130617.

Xu, G., Zhou, J., Liu, K., et al., 2025. Macrophage-augmented intestinal organoids model virus-host interactions in enteric viral diseases and facilitate therapeutic development. Nat. Commun. 16 (1), 4475. https://doi.org/10.1038/s41467-025-59639-9.

Xuan, L., Luo, J., Qu, C., et al., 2024. Predictive metabolomic signatures for safety assessment of three plastic nanoparticles using intestinal organoids. Sci. Total Environ. 913, 169606. https://doi.org/10.1016/j.scitotenv.2023.169606.

Yan, Z., Liu, Y., Zhang, T., Zhang, F., Ren, H., Zhang, Y., 2022. Analysis of microplastics in human feces reveals a correlation between fecal microplastics and inflammatory bowel disease status. Environ. Sci. Technol. 56 (1), 414–421. https://doi.org/10.1021/acs.est.1c03924.

Yin, Y., Bijvelds, M., Dang, W., et al., 2015. Modeling rotavirus infection and antiviral therapy using primary intestinal organoids. Antiviral Res. 123, 120–131. https://doi.org/10.1016/j.antiviral.2015.09.010.

Zhang, G., Cao, G., Luo, R.-H., et al., 2022. Microplastics interact with SARS-CoV-2 and facilitate host cell infection. Environ. Sci. Nano 9 (8), 2653–2664. https://doi.org/10.1039/d2en00019a.

Zhang, K., Su, J., Xiong, X., Wu, X., Wu, C., Liu, J., 2016. Microplastic pollution of lakeshore sediments from remote lakes in Tibet plateau, China. Environ. Pollut. 219, 450–455. https://doi.org/10.1016/j.envpol.2016.05.048.

Zhang, F., Wang, Z., Vijver, M.G., Peijnenburg, W.J.G.M., 2022. Theoretical investigation on the interactions of microplastics with a SARS-CoV-2 RNA fragment and their potential impacts on viral transport and exposure. Sci. Total Environ. 842, 156812. https://doi.org/10.1016/j.scitotenv.2022.156812.